Development of a diagnostic model for esophageal achalasia assessed by esophageal high-resolution manometry using artificial intelligence

MAIKO TABUCHI[1,2], YASUHIKO NAKAO[2], HITOMI MINAMI[2,3], HIROKO INOMATA[2], JUNYA SHIOTA[2], TARO AKASHI[2], KEIICHI HASHIGUCHI[2,4], MOTO KITAYAMA[2], KAYOKO MATSUSHIMA[2], NAOYUKI YAMAGUCHI[2,4], YUKO AKAZAWA[1,2] and HISAMITSU MIYAAKI[2]

[1]Department of Histology and Cell Biology, Nagasaki University Graduate School of Biomedical Sciences, Nagasaki, Nagasaki 852-8523, Japan; [2]Department of Gastroenterology and Hepatology, Nagasaki University Graduate School of Biomedical Sciences, Nagasaki, Nagasaki 852-8501, Japan; [3]Department of Internal Medicine, Tachibana Bay Clinic, Nagasaki, Nagasaki 851-0123, Japan; [4]Department of Endoscopy, Nagasaki University Hospital, Nagasaki, Nagasaki 852-8501, Japan

Received June 20, 2025; Accepted December 12, 2025

DOI: 10.3892/etm.2026.13071

Abstract. Esophageal high-resolution manometry (HRM) is an important tool for diagnosing and assessing esophageal achalasia. Artificial intelligence (AI)-assisted HRM image processing has the potential to aid in the diagnosis of esophageal achalasia. However, addressing the challenges associated with the 'black-box' problem is important. In the present study, an automated system that utilizes AI with class-activation maps to highlight diagnostic areas in HRM images was developed. A total of 211 HRM images, which led to the diagnosis of controls and patients with achalasia, were used to train the system using Resnet34, a convolutional neural network model. The diagnoses included normal, type I achalasia, type II achalasia, type III achalasia and hypercontractile esophagus based on the Chicago classification v3.0 for esophageal motility disorders. A gradient class activation map (Grad-CAM) technique was used. The discrimination model for the control and achalasia groups yielded a 100% correct response rate for evaluating the validation images (n=30). Grad-CAM analysis revealed that the model focused on the area around the lower esophageal sphincter pressure in type 1 achalasia for differentiation, closely aligning with expert perspectives. An AI-based HRM imaging assistance system may not only support physicians in distinguishing esophageal motility disorders with improved diagnostic accuracy but also serve as a novel tool that provides deeper clinical insights and highlights key interpretative features in HRM evaluations. Further large-scale validation is required to confirm its clinical utility.

Correspondence to: Dr Yasuhiko Nakao, Department of Gastroenterology and Hepatology, Nagasaki University Graduate School of Biomedical Sciences, 1-7-1 Sakamoto, Nagasaki, Nagasaki 852-8501, Japan
E-mail: yasu.nakao@nagasaki-u.ac.jp

Key words: high-resolution manometry, artificial intelligence, achalasia, esophageal motility disorder

Introduction

Achalasia is a rare motility disorder of the esophagus characterized by dysphagia, chest pain, and weight loss (1,2). It has an annual incidence of one in 100,000 individuals and a prevalence of 10 in 100,000 individuals, and occurs equally in male and female patients (3). Although the exact cause remains largely unknown, a combination of genetic and environmental factors, such as viral infection-mediated immune reactions, may lead to ganglionitis and the loss of esophageal neurons (1,4,5). Achalasia is defined by a combination of symptoms, endoscopic findings, esophagography, and esophageal high-resolution manometry (HRM) (2,6).

Although the underlying causes and variations in esophageal motility disorders remain largely unknown, HRM has emerged as an essential tool for defining and detecting these disorders (2,6). The Chicago classification using HRM is helpful for the diagnosis and pretreatment evaluation of esophageal achalasia (7). The integrated relaxation pressure (IRP) indicates the elevation of the lower esophageal sphincter (LES) pressure for several seconds after swallowing (8). In the Chicago classification, this value serves as the starting point for developing the algorithm, indicating an abnormal motility disorder (7). However, relying solely on the IRP in the algorithm is often inconsistent with the clinical diagnosis (9); therefore, a comprehensive assessment by a physician, incorporating other modalities, is usually necessary. The IRP value, essential for diagnosis, is dynamic and influenced by factors such as diaphragmatic activity, LES function, intrabolus pressure, and catheter positioning (10,11). An accurate interpretation requires a comprehensive assessment that extends beyond the numerical values (11). Interpreting HRM poses significant challenges and requires specialized expertise for an accurate diagnosis. This exclusive reliance on specialists

for this diagnostic procedure has led to delays in identifying esophageal motility disorders, such as achalasia.

Artificial intelligence (AI) can alleviate issues associated with the clinical interpretation of HRM. Due to the rarity of this disease, few studies have assessed AI in patients with achalasia. Kou *et al* (12) first demonstrated a deep learning-based model for diagnosing achalasia using HRM images, employing a variational autoencoder (VAE). Surdea-Blaga *et al* (13) demonstrated the classification of swallowing disorders using the DenseNet201 convolutional neural network (CNN) architecture combined with the automated Chicago classification, yielding 86% accuracy without human intervention. Although AI-based tools are emerging in the medical field, a black-box problem arises: they do not reveal how or why they were concluded. In AI-based achalasia, whether AI focuses on the same area as clinicians remains unclear.

In this study, we validated an automated diagnostic system using AI to assess HRM. In addition, we utilized a gradient class activation map (Grad-CAM) to evaluate the features of HRM, where the AI focused on distinguishing achalasia from other esophageal motor disorders.

Materials and methods

Data collection and ethical approval. The research implementation system was conducted at a single center. This retrospective study was approved by the Nagasaki University Hospital Research Ethics Committee. This retrospective study was approved by the ethics review board and the requirement for informed consent was waived.

Data pre-processing. A total of 211 HRM images were de-identified to protect patient confidentiality and were collected between December 2018 and August 2022 at the Nagasaki University Hospital. Typical HRM images obtained from patients with achalasia who underwent POEM were used as achalasia images, whereas HRM images from asymptomatic individuals were used as normal controls. Images that were unclear or diagnostically ambiguous were excluded from the analyses. Before submitting the images for model training, each image was cropped to remove the patient identification, machine settings, annotations, and scale bars. High-resolution esophageal manometry was performed using the Starlet system (Star Medical, Tokyo, Japan).

We selected tracings from ten test swallows for analysis (n=22 patients; 211 images): achalasia type I, 67 images; achalasia type II, 30 images; achalasia type III, 9 images; hypercontractile esophagus, 20 images; and normal esophageal motility, 97 images. We used the raw data, which contained only the markers mentioned above (vertical white lines) preceding each wet swallow. The manometry software enabled the storage of 60 s long images of the recordings, which represented the raw images. The region of interest (wet swallowing) was marked with a white vertical line during the procedure. For each patient, we created a folder with ten images, with each image representing a test swallow.

Each set is assigned a diagnostic category. We used five diagnostic categories as follows: normal, type I achalasia, type II achalasia, type III achalasia, and hypercontractile esophagus, based on the Chicago v3.0 classification for esophageal motility disorders (7).

Developing a deep learning algorithm. Achalasia was predicted by using the CNN. The ResNet-34 network was used as the backbone of the encoder network to encode the downsampling layer of the image. The model was trained using Python 3.8 (Python Software Foundation, Beaverton, OR, USA), Pytorch 1.8.1 (The Linux Foundation), and an Nvidia RTX A6000 graphics card. The achalasia prediction training process utilized a mean-squared error loss function and an Adam optimizer with a batch size of 4; the learning rate decreased linearly from $5e^{-4}$ to $1e^{-6}$.

Grad-CAM method. Grad-CAM was used to reconstruct the image and localize intensive areas for feature extraction. This method identifies the image features used by a CNN to perform the decision-making process, thereby enabling an understanding of the predictive features determined by the trained model. We used Grad-CAM to identify key abnormal features in the dataset. Regions with high feature extraction intensities were assumed to be key points in identifying anomalies.

Dimensions reduction analysis. Principal component analysis (PCA) and three-dimensional t-distributed stochastic neighbor embedding (3D-tSNE) were used for feature analysis of the entire image (14). PCA was used to reduce the dimensions. A TensorBoard Embedding Projector, which offers 3D-tSNE views, was used to compute the top ten principal components. These components were projected onto a combination of three components. The most popular nonlinear dimensionality reduction technique is t-SNE (15).

Statistical analysis. Testing accuracy, sensitivity, and specificity, as calculated from the confusion matrix, were used to evaluate the models. The receiver operating characteristic (ROC) curve, which is a graphical plot highly correlated with the confusion matrix, was also used as an evaluation index. Diagnostic accuracy based on the confusion matrix was calculated as follows: (true positives + true negatives)/(true positives + true negatives + false positives + false negatives). All statistical analyses were performed using the R statistical software (version 4.1.1; The R Foundation for Statistical Computing, Vienna, Austria). Statistical significance was set at $P<0.05$.

Results

All patients with achalasia included in the study were treatment-naïve and had no prior interventions, such as balloon dilation, Heller myotomy, or peroral endoscopic myotomy (POEM) (Table I). The training process for the achalasia-2CNN is illustrated in Fig. 1. First, we developed an achalasia prediction model using HRM with CNN (Fig. 1). The ResNet-34 model, which has already been proven to be versatile, was used for transfer learning. Two hundred images were divided into training and validation datasets, and a CNN based primarily on the PyTorch framework was used. With training, the accuracy of the training and validation sets increased, and the loss value decreased. The accuracy of the validation set was highest in the fourth epoch of training (Fig. 2, left

Table I. Patient characteristics.

Characteristics	Achalasia (n=12)	Normal (n=9)
Age, years	41 (16-89)	72 (50-82)
Sex (male)	7 (58)	6 (67)
Eckardt score (normal, ≤3)	7 (1-10)	0 (0-0)
Prior treatment (yes)	0 (0)	0 (0)
IRP, mmHg (normal, ≤25 mmHg)	23.6 (0.6-55.0)	10.4 (3.6-18.5)
Maximum DCI, mmHg·sec·cm (normal range, 450-8,000 mmHg·sec·cm)	796.1 (397.0-493,490.0)	1,701.1 (238.1-3,713.1)

Data are presented as the median (range) or n (%). IRP, integrated relaxation pressure; DCI, distal contractile integral.

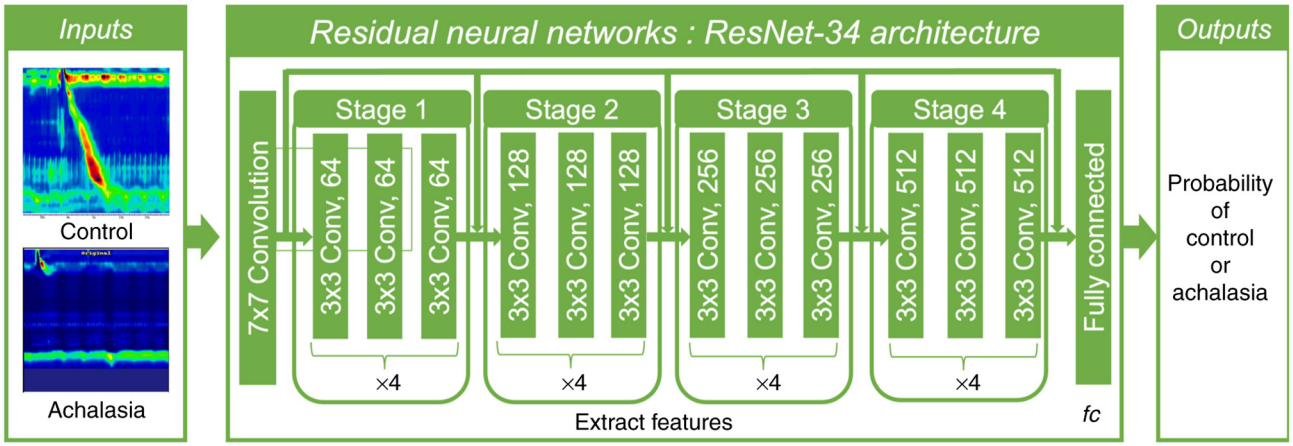

Figure 1. Learning process involving ResNet-34. Standard high-resolution manometry images and images from patients with achalasia were provided as inputs and labeled as 'Control' and 'Achalasia', respectively. The output represents the probability of the validation image being classified as either 'Control' or 'Achalasia'. Conv, convolutional layer; fc, fully connected layer.

panel). Fig. 2 (right panel) shows that the confusion matrix of the achalasia-CNN optimal model was 100% accurate for the external test set, with both sensitivity and specificity reaching 100%. The receiver operating characteristic (ROC) curve, area under the curve (AUC), sensitivity, and specificity are shown in Table SI and Fig. S1.

Owing to the nearly 100% correct response rate, and despite the small dataset, PCA was performed on the characteristics of the dataset. The HRM of patients with achalasia was distributed mainly on the left side of Fig. 3, indicating that the features of each HRM image differed between the controls and patients with achalasia. Similarly, a 3D-tSNE analysis, a dimensionality removal method, was performed (Fig. 4), which showed that the achalasia group could be further subdivided into several groups, suggesting the possibility of extracting features using an achalasia-type classification.

The difference in HRM features between the controls and patients with achalasia, even in the absence of a large number of HRM images, suggests that deep learning may be predominantly predictive of the disease. Thus, predictors of each type of achalasia were developed using the same methods.

Next, we developed an achalasia-type prediction model using HRM with deep learning. The confusion matrix in Fig. 5 shows the predictions for each type. Of the 22 validation datasets, two were incorrectly classified as type 1 for type 2 achalasia; however, the others were correctly classified (Fig. 6). These results demonstrate that deep learning can achieve high accuracy rates in HRM diagnosis, even with small datasets. The comprehensive performance metrics are presented in Table SII and Fig. S2.

The legends visualized using Grad-CAM are shown in Fig. 7. The images were reviewed by two achalasia diagnosticians, primarily based on the diagnosis, with high-signal images in the heatmap of the LES pressure region, which is a crucial area for achalasia diagnosis.

When reexamining the areas of focus of Grad-CAM, we found that pan-esophageal pressurization, which is continuous with upper esophageal sphincter contraction, is a feature of type 2 achalasia (Fig. S3). Interestingly, these features are not found in type 1 achalasia, suggesting that they may be imaging features of type 2 achalasia.

Discussion

In recent years, multimodal therapy combining surgical resection with chemotherapy, chemoradiotherapy, and immunotherapy has become widely adopted for malignant esophageal diseases such as esophageal cancer, leading

Epoch	Train_loss	Valid_loss	Accuracy	Time
0	0.977863	0.383664	0.933333	00:06

Epoch	Train_loss	Valid_loss	Accuracy	Time
0	0.553477	0.174930	0.966667	00:04
1	0.461644	0.194452	0.933333	00:03
2	0.479477	0.024958	1.000000	00:03
3	0.463008	0.037218	1.000000	00:04

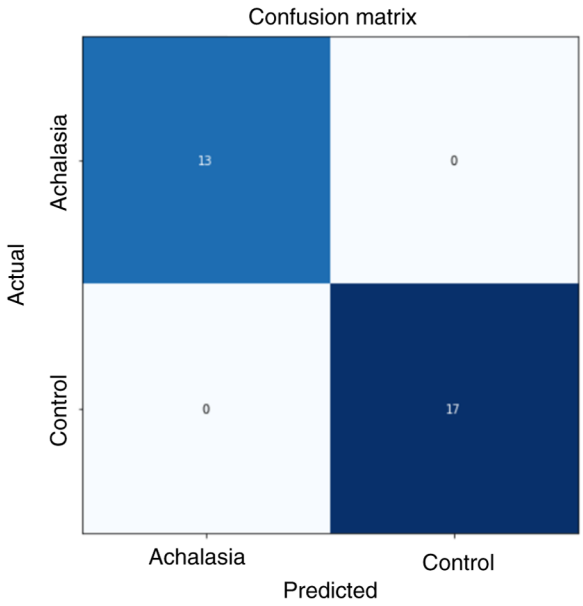

Figure 2. Training a ResNet-34 model to distinguish achalasia from normal esophagus. The left panel shows the learning process, which was repeated four times using ResNet-34. The right panel shows validation data with 100% accuracy across the validation dataset. 'Train loss' and 'valid loss' indicate the loss values computed for the training and validation datasets, respectively. The time indicates the duration required for each epoch (mm:ss).

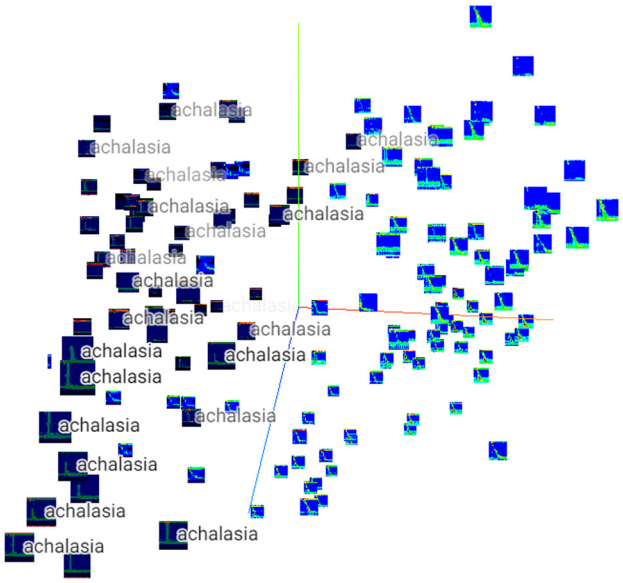

Figure 3. PCA. Images from PCA using the TensorBoard software. Black panels represent achalasia cases, whereas blue panels represent control cases. The spatial separation between the two groups reflects differences in the learned feature representations. The spatial separation between the two groups reflects the difference in the learned feature representations. PCA, principal component analysis.

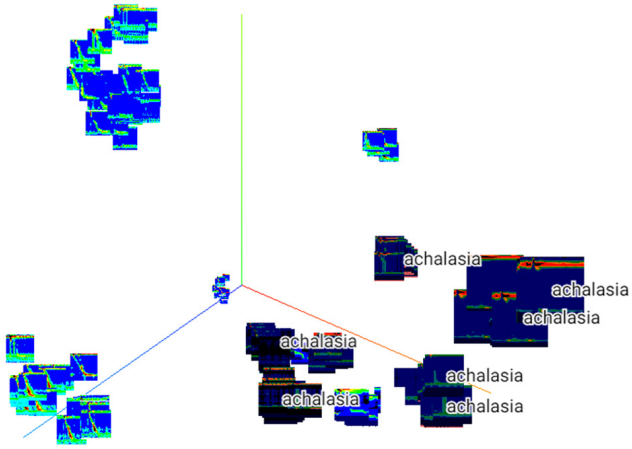

Figure 4. Analysis with 3D-tSNE. The figure shows a combination of principal component analysis and 3D-tSNE analysis. Black panels represent achalasia cases, whereas blue panels represent control cases. Notably, an additional subdivision within the achalasia category was observed, suggesting a more detailed characterization of the data. 3D-tSNE, three-dimensional t-distributed stochastic neighbor embedding.

to significant improvements in patient prognosis (16-19). Furthermore, advances in endoscopic diagnosis have enabled earlier detection of esophageal squamous cell carcinoma (ESCC), and endoscopic submucosal dissection (ESD) for early lesions has markedly improved prognosis (20,21).

In contrast, benign esophageal motility disorders, such as achalasia, require precise functional evaluation and have often been overlooked due to the complexity of diagnostic tools and a limited comprehensive understanding of these conditions (22,23). HRM serves as a highly valuable functional imaging examination tool, and its diagnostic accuracy and progression are pivotal for future elucidation and treatment of the underlying causes of esophageal motility disorders (1,9,24). Once achalasia is accurately diagnosed using HRM, patients can experience marked symptom improvement through appropriate therapeutic interventions, such as peroral endoscopic myotomy (POEM) or Heller-Dor surgery (1,25,26).

However, the diagnosis of esophageal motility disorders using HRM can be highly challenging. Even in achalasia, cases with normal IRP values (9 out of 12 patients, within the normal range of ≤25 mmHg) were observed in our cohort, and such patients cannot always be accurately diagnosed, even when the Chicago Classification is applied. Several studies

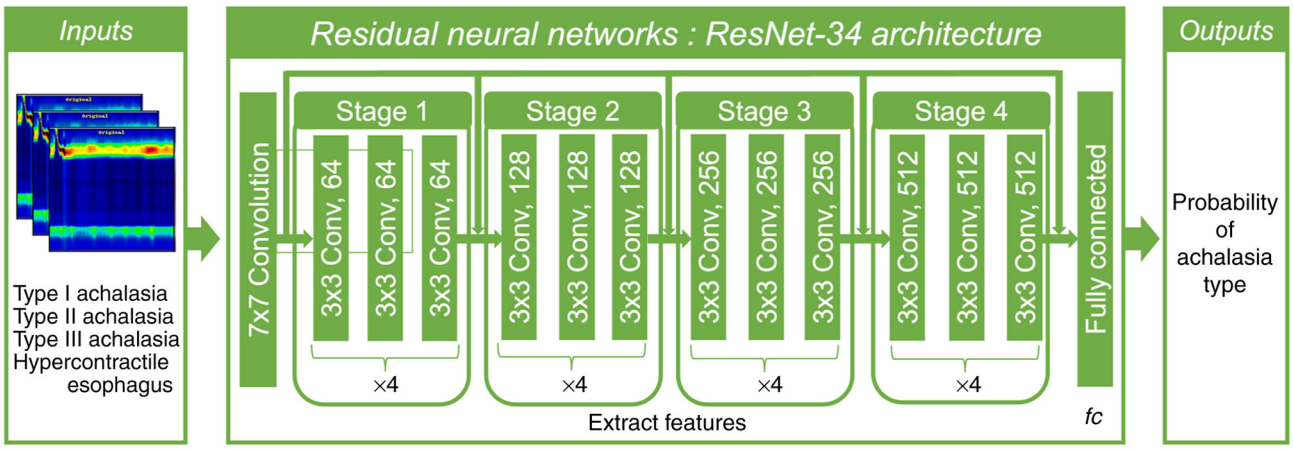

Figure 5. Training of a ResNet-34 model for classification of achalasia subtypes and hypercontractile esophagus. The resulting outputs comprised the probabilities of achalasia types and hypercontractile esophageal classifications based on validation images. Conv, convolutional layer; fc, fully connected layer.

Epoch	Train_loss	Valid_loss	Accuracy	Time
0	2.072391	0.640538	0.681818	00:14

Epoch	Train_loss	Valid_loss	Accuracy	Time
0	1.097691	0.707897	0.772727	00:03
1	0.858385	0.402162	0.818182	00:03
2	0.852989	0.334026	0.954545	00:03
3	0.834208	0.373110	0.909091	00:03

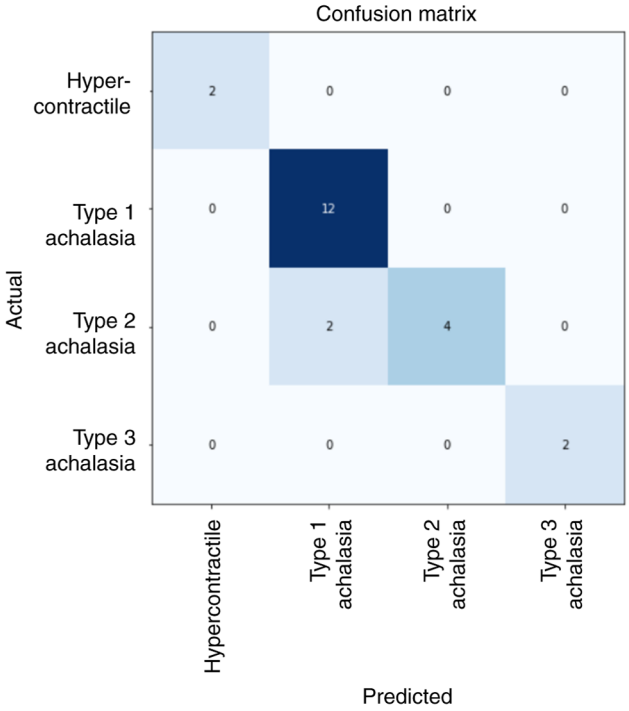

Figure 6. Training a ResNet-34 model to distinguish achalasia typing. The left panel shows the learning process repeated four times. The right panel shows the validation data, with an accuracy of 90.9% observed across the validation dataset for the classification of achalasia type and hypercontractile esophagus. 'Train loss' and 'valid loss' indicate the loss values computed for the training and validation datasets, respectively. The time indicates the duration required for each epoch (mm:ss).

have reported the presence of achalasia with normal IRP values. Proposed mechanisms include impaired esophagogastric junction opening due to fibrotic changes of the LES (27), as well as advanced age or pronounced esophageal tortuosity and dilatation (28). In addition, when using the Starlet catheter, Type I achalasia may present with lower IRP values than expected (29). Therefore, diagnosing esophageal motility disorders based on HRM topography, rather than relying solely on numerical indices such as IRP, is essential. However, describing and quantifying the image features that serve as diagnostic criteria remains challenging. The present results demonstrate that AI-assisted diagnosis can be a valuable approach for identifying achalasia.

Rare esophageal motility disorders, such as distal esophageal spasm (DES) and esophagogastric junction outflow obstruction (EGJOO), have been reported in previous studies (30). Achalasia is characterized by a selective loss of inhibitory myenteric neurons in the distal esophagus and LES, resulting in impaired esophagogastric junction (EGJ) relaxation and loss of normal peristalsis (31). High-resolution manometry shows an elevated IRP with absent peristalsis, with type I-III subtypes distinguished by the presence of panesophageal pressurization or premature spastic contractions. In contrast, EGJ outflow obstruction is defined in the Chicago Classification as an elevated median IRP with preserved- or only weakly impaired-peristalsis, and is considered a heterogeneous manometric pattern that may

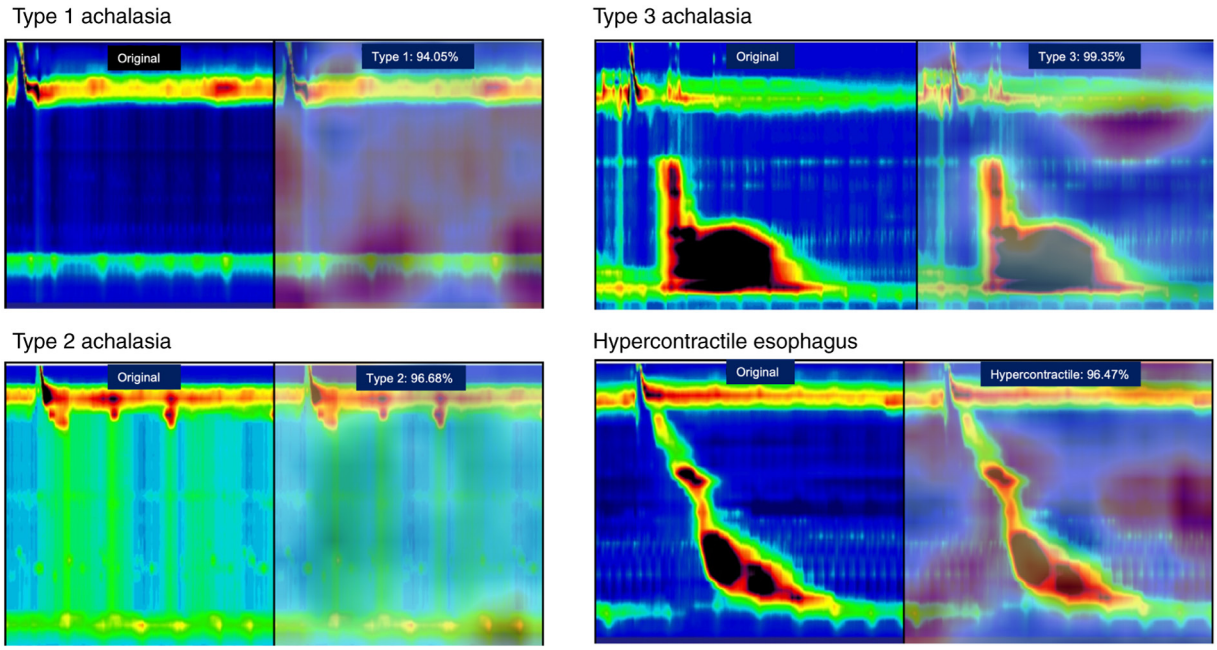

Figure 7. Grad-CAM visualization highlighting regions contributing to AI-based classification. Grad-CAM visualizations show hotspots in the right panels, representing regions that the AI focused on to distinguish achalasia from control images. These hotspots, highlighted by the AI, signify areas where the disease images differ from the control images and the percentage indicates the predicted probability for each class obtained from the softmax output. Grad-CAM, gradient class activation map program; AI, artificial intelligence.

reflect early or variant achalasia, mechanical obstruction (e.g., hiatal hernia, stricture, malignancy), or post-surgical changes rather than a single primary motility disorder (32). Accordingly, the current Chicago Classification v4.0 requires not only HRM findings but also supportive evidence from endoscopy, timed barium esophagram, or functional lumen imaging probe (FLIP) to distinguish clinically relevant EGJOO from incidental manometric abnormalities (33). Distal esophageal spasm (DES) is thought to result from an imbalance between excitatory and inhibitory innervation confined mainly to the distal esophagus; HRM in DES demonstrates premature contractions (distal latency <4.5 s) in ≥20% of swallows with normal EGJ relaxation, typically in patients with dysphagia or non-cardiac chest pain (34). Thus, while all three conditions share abnormalities in inhibitory neural control of the esophagus, achalasia is defined by impaired EGJ relaxation with absent peristalsis, EGJOO by impaired EGJ relaxation with preserved peristalsis, and DES by premature distal contractions with normal EGJ relaxation. In HRM, premature contractions can also be observed in type III achalasia, and some achalasia cases may present with normal IRP values, making it easily confused with DES. Moreover, EGJOO cannot be accurately diagnosed based solely on HRM findings; additional evaluations, such as endoscopy, timed barium esophagram, or FLIP, are required to confirm true obstruction. Therefore, we considered DES and EGJOO to be inappropriate as the initial targets for AI model development.

In this study, we developed and validated an achalasia prediction and classification model using HRM with deep learning. To the best of our knowledge, this is the first time AI has demonstrated the potential to support medical practice by visualizing AI prediction sites using Grad-CAM and reevaluating them from a physician's perspective. Few reports are available on the use of deep learning for HRM images. For example, models based on VAE and DenseNet201 (35) have been shown to achieve high accuracy rates, reaching approximately 93% in classifying esophageal motility disorders (36). In addition, Kou *et al* (37) reported that a Long Short-Term Memory (LSTM) model achieved a correct classification rate of 88% for the Chicago Classification using HRM images. We employed a relatively generic convolutional neural network, ResNet-34 (38), with transfer learning for HRM image classification, achieving a correct classification rate of 95%, consistent with prior deep-learning studies. To investigate the underlying cause, we conducted PCA and 3D-tSNE analyses, which indicated that the discriminative challenge could be advantageous for AI in distinguishing between normal HRM and achalasia cases, given the fundamental differences in the image features. Although the internal validation yielded AUCs of 1.000 and very high sensitivity and specificity, these figures should be regarded as optimistic estimates rather than evidence of perfect clinical performance. The validation sets were small (22 cases for the multiclass task and 30 cases for the binary task), and with such sample sizes, an empirically perfect ROC curve can occur when the model ranks all cases correctly in a single split. In addition, we fine-tuned a pre-trained ResNet-34 model on data from a single source, which increases the risk of overfitting to the local data distribution. Therefore, the present results should be interpreted as showing that the model can separate these particular data well, and not that it will achieve 100% accuracy in broader practice. Future studies should include repeated cross-validation and, more importantly, external validation in a larger and more heterogeneous cohort.

Previous studies have reported that AI prediction of HRM images is helpful for the Chicago classification of achalasia, achieving a high accuracy level of 81-93% (37,39). In this

study, our validation dataset yielded a classification accuracy of 95% for the Chicago Classification groups. Furthermore, we not only developed a classification model but also applied Grad-CAM to visualize the regions contributing to the AI's predictions and reviewed all images from the perspective of esophageal specialists. The Grad-CAM results also focused on LES pressure in the HRM image, demonstrating that the LES plays a crucial role in representing pathological function, as mentioned previously (40). These findings are valuable for guiding treatment choices. Grad-CAM images can be instrumental in determining whether to cut or preserve the LES during procedures such as peroral endoscopic myotomy, diffuse esophageal spasm, and hypercontractile esophagus, which are collectively referred to as esophageal motility disorders (30).

In the future, we plan to introduce our developed model in medical practice and investigate its potential not only for the identification of achalasia but also as a tool for medical education, supporting residents and other physicians through AI-assisted diagnostics.

A limitation of HRM is that it is primarily used to evaluate rare diseases, making validation with large datasets and balanced case designs challenging. Therefore, validation on large datasets and with a balanced case design is difficult. Although a discriminator and classification model for achalasia was developed in this study, further development and validation of the model were constrained by the lack of sufficient training data for other rare esophageal diseases. Future directions may include the implementation of abnormality-detection models based on generative adversarial networks, which hold promise for addressing these limitations.

In conclusion, our AI-based HRM assistance system not only enhances diagnostic accuracy but also offers clinicians new insights and interpretative perspectives for HRM evaluation. Further large-scale studies are required to validate its utility.

Acknowledgements

Not applicable.

Funding

No funding was received.

Availability of data and materials

The data generated in the present study are not publicly available because they contain information that could compromise the privacy of research participants, but may be requested from the corresponding author.

Authors' contributions

MT and YN conducted the experiments and wrote the manuscript. HMin, NY, YA and HMiy made substantial contributions to the conception and design of the study. MT, HI, JS, TA, KH, MK, KM and HMin contributed to acquisition and analysis of data. NY, YA and HMiy critically revised the manuscript for important intellectual content. HMin, JS and YN confirm the authenticity of all the raw data. All authors have read and approved the final version of the manuscript.

Ethics approval and consent to participate

The study protocol was reviewed and approved by the Nagasaki University Hospital Research Ethics Committee (approval no. 23041703-2; Nagasaki, Japan), and the need for informed consent was waived. The hospital website ensures that patients have the right to refuse to share information through an opt-out system.

Patient consent for publication

Patient consent for publication was obtained using an opt-out approach, whereby the study information was publicly disclosed, as approved by the Nagasaki University Hospital Research Ethics Committee.

Competing interests

The authors declare that they have no competing interests.

Use of artificial intelligence tools

During the preparation of this work, artificial intelligence tools were used to improve the readability and language of the manuscript or to generate images, and subsequently, the authors revised and edited the content produced by the artificial intelligence tools as necessary, taking full responsibility for the ultimate content of the present manuscript.

References

1. Boeckxstaens GE, Zaninotto G and Richter JE: Achalasia. Lancet 383: 83-93, 2014.
2. Vaezi MF, Pandolfino JE, Yadlapati RH, Greer KB and Kavitt RT: ACG clinical guidelines: Diagnosis and management of achalasia. Am J Gastroenterol 115: 1393-1411, 2020.
3. Vaezi MF, Pandolfino JE and Vela MF: ACG clinical guideline: Diagnosis and management of achalasia. Am J Gastroenterol 108: 1238-1249, 1250, 2013.
4. Naik RD, Vaezi MF, Gershon AA, Higginbotham T, Chen JJ, Flores E, Holzman M, Patel D and Gershon MD: Association of achalasia with active varicella zoster virus infection of the esophagus. Gastroenterology 161: 719-721.e2, 2021.
5. Gaber CE, Cotton CC, Eluri S, Lund JL, Farrell TM and Dellon ES: Autoimmune and viral risk factors are associated with achalasia: A case-control study. Neurogastroenterol Motil 34: e14312, 2022.
6. Yamasaki T, Tomita T, Mori S, Takimoto M, Tamura A, Hara K, Kondo T, Kono T, Tozawa K, Ohda Y, *et al*: Esophagography in patients with esophageal achalasia diagnosed with high-resolution esophageal manometry. J Neurogastroenterol Motil 24: 403-409, 2018.
7. Kahrilas PJ, Bredenoord AJ, Fox M, Gyawali CP, Roman S, Smout AJ and Pandolfino JE; International High Resolution Manometry Working Group: The Chicago Classification of esophageal motility disorders, v3.0. Neurogastroenterol Motil 27: 160-174, 2015.
8. do Carmo GC, de Assis Mota G, da Silva Castro Perdoná G and de Oliveira RB: Integrated relaxation pressure and its diagnostic ability may vary according to the conditions used for HREM recording. Dysphagia 39: 746-756, 2024.
9. Cha B and Jung KW: Diagnosis of dysphagia: High resolution manometry & EndoFLIP. Korean J Gastroenterol 77: 64-70, 2021 (In Korean).

10. Czako Z, Surdea-Blaga T, Sebestyen G, Hangan A, Dumitrascu DL, David L, Chiarioni G, Savarino E and Popa SL: Integrated relaxation pressure classification and probe positioning failure detection in high-resolution esophageal manometry using machine learning. Sensors (Basel) 22: 253, 2021.
11. Gong EJ: Integrated relaxation pressure during swallowing: An Ever-changing metric. J Neurogastroenterol Motil 27: 151-152, 2021.
12. Kou W, Carlson DA, Baumann AJ, Donnan E, Luo Y, Pandolfino JE and Etemadi M: A deep-learning-based unsupervised model on esophageal manometry using variational autoencoder. Artif Intell Med 112: 102006, 2021.
13. Surdea-Blaga T, Sebestyen G, Czako Z, Hangan A, Dumitrascu DL, Ismaiel A, David L, Zsigmond I, Chiarioni G, Savarino E, *et al*: Automated Chicago classification for esophageal motility disorder diagnosis using machine learning. Sensors (Basel) 22: 5227, 2022.
14. Luus F, Khan N and Akhalwaya I: Active learning with tensorboard projector. arXiv.org, 2019.
15. Van der Maaten L and Hinton G: Visualizing data using t-SNE. J Mach Learn Res 9: 2579-2605, 2008.
16. Kanamori K, Koyanagi K, Ozawa S, Yamamoto M, Ninomiya Y, Yatabe K, Higuchi T and Tajima K: Multimodal therapy for esophageal squamous cell carcinoma according to TNM staging in Japan-a narrative review of clinical trials conducted by Japan clinical oncology group. Ann Esophagus 6: 32, 2023.
17. Koyanagi K, Kanamori K, Ninomiya Y, Yatabe K, Higuchi T, Yamamoto M, Tajima K and Ozawa S: Progress in multimodal treatment for advanced esophageal squamous cell carcinoma: Results of multi-institutional trials conducted in Japan. Cancers (Basel) 13: 51, 2020.
18. Higuchi T, Shoji Y, Koyanagi K, Tajima K, Kanamori K, Ogimi M, Yatabe K, Ninomiya Y, Yamamoto M, Kazuno A, *et al*: Multimodal treatment strategies to improve the prognosis of locally advanced thoracic esophageal squamous cell carcinoma: A narrative review. Cancers (Basel) 15: 10, 2022.
19. Bolger JC, Donohoe CL, Lowery M and Reynolds JV: Advances in the curative management of oesophageal cancer. Br J Cancer 126: 706-717, 2022.
20. Yang H, Wang F, Hallemeier CL, Lerut T and Fu J: Oesophageal cancer. Lancet 404: 1991-2005, 2024.
21. Nishizawa T and Suzuki H: Long-term outcomes of endoscopic submucosal dissection for superficial esophageal squamous cell carcinoma. Cancers (Basel) 12: 2849, 2020.
22. Averbukh LD and Tadros M: The role of automatically generated Chicago classification in delayed achalasia diagnosis. ACG Case Rep J 7: e00345, 2020.
23. Müller M, Förschler S, Wehrmann T, Marini F, Gockel I and Eckardt AJ: Atypical presentations and pitfalls of achalasia. Dis Esophagus 36: doad029, 2023.
24. Richter JE: High-resolution manometry in diagnosis and treatment of achalasia: Help or hype. Curr Gastroenterol Rep 16: 420, 2014.
25. Inoue H, Minami H, Kobayashi Y, Sato Y, Kaga M, Suzuki M, Satodate H, Odaka N, Itoh H and Kudo S: Peroral endoscopic myotomy (POEM) for esophageal achalasia. Endoscopy 42: 265-271, 2010.
26. Schlottmann F and Patti MG: Esophageal achalasia: Current diagnosis and treatment. Expert Rev Gastroenterol Hepatol 12: 711-721, 2018.
27. Sato H, Takahashi K, Mizuno KI, Hashimoto S, Yokoyama J and Terai S: A clinical study of peroral endoscopic myotomy reveals that impaired lower esophageal sphincter relaxation in achalasia is not only defined by high-resolution manometry. PLoS One 13: e0195423, 2018.
28. Kim E, Yoo IK, Yon DK, Cho JY and Hong SP: Characteristics of a subset of achalasia with normal integrated relaxation pressure. J Neurogastroenterol Motil 26: 274-280, 2020.
29. Kawami N, Hoshino S, Hoshikawa Y, Takenouchi N, Hanada Y, Tanabe T, Goto O, Kaise M and Iwakiri K: Validity of the cutoff value for integrated relaxation pressure used in the Starlet high-resolution manometry system. J Nippon Med Sch 86: 322-326, 2020.
30. Morley TJ, Mikulski MF, Rade M, Chalhoub J, Desilets DJ and Romanelli JR: Per-oral endoscopic myotomy for the treatment of non-achalasia esophageal dysmotility disorders: Experience from a single high-volume center. Surg Endosc 37: 1013-1020, 2023.
31. Rogers AB, Rogers BD and Gyawali CP: Pathophysiology of achalasia. Ann Esophagus 3: 27, 2020.
32. Rohof WOA and Bredenoord AJ: Chicago classification of esophageal motility disorders: Lessons learned. Curr Gastroenterol Rep 19: 37, 2017.
33. Yadlapati R, Kahrilas PJ, Fox MR, Bredenoord AJ, Prakash Gyawali C, Roman S, Babaei A, Mittal RK, Rommel N, Savarino E, *et al*: Esophageal motility disorders on high-resolution manometry: Chicago classification version 4.0©. Neurogastroenterol Motil 33: e14058, 2021.
34. Fox MR, Sweis R, Yadlapati R, Pandolfino J, Hani A, Defilippi C, Jan T and Rommel N: Chicago classification version 4.0© technical review: Update on standard high-resolution manometry protocol for the assessment of esophageal motility. Neurogastroenterol Motil 33: e14120, 2021.
35. Huang G, Liu Z, Pleiss G, van der Maaten L and Weinberger KQ: Convolutional networks with dense connectivity. IEEE Trans Pattern Anal Mach Intell 44: 8704-8716, 2022.
36. Popa SL, Surdea-Blaga T, Dumitrascu DL, Chiarioni G, Savarino E, David L, Ismaiel A, Leucuta DC, Zsigmond I, Sebestyen G, *et al*: Automatic diagnosis of high-resolution esophageal manometry using artificial intelligence. J Gastrointestin Liver Dis 31: 383-389, 2022.
37. Kou W, Galal GO, Klug MW, Mukhin V, Carlson DA, Etemadi M, Kahrilas PJ and Pandolfino JE: Deep learning-based artificial intelligence model for identifying swallow types in esophageal high-resolution manometry. Neurogastroenterol Motil 34: e14290, 2022.
38. He K, Zhang X, Ren S and Sun J: Deep residual learning for image recognition. arXiv [csCV]: 770-778, 2015.
39. Kou W, Carlson DA, Baumann AJ, Donnan EN, Schauer JM, Etemadi M and Pandolfino JE: A multi-stage machine learning model for diagnosis of esophageal manometry. Artif Intell Med 124: 102233, 2022.
40. Cohen S, Lipshutz W and Hughes W: Role of gastrin supersensitivity in the pathogenesis of lower esophageal sphincter hypertension in achalasia. J Clin Invest 50: 1241-1247, 1971.